

# Confronting new NICER mass-radius measurements with phase transition in dense matter and twin compact stars

Jia Jie Li<sup>a</sup> Armen Sedrakian<sup>b,c</sup> Mark Alford<sup>d</sup>

<sup>a</sup>School of Physical Science and Technology, Southwest University, Chongqing 400715, China

<sup>b</sup>Frankfurt Institute for Advanced Studies, D-60438 Frankfurt am Main, Germany

<sup>c</sup>Institute of Theoretical Physics, University of Wrocław, 50-204 Wrocław, Poland

<sup>d</sup>Department of Physics, Washington University, St. Louis, Missouri 63130, USA

E-mail: [jjajeli@swu.edu.cn](mailto:jjajeli@swu.edu.cn); [sedrakian@fias.uni-frankfurt.de](mailto:sedrakian@fias.uni-frankfurt.de); [alford@physics.wustl.edu](mailto:alford@physics.wustl.edu)

## Abstract.

The (re)analysis of data on the X-ray emitting pulsars PSR J0030+0451 and J0740+6620, as well as new results on PSR J0437-4715 and J1231-1411, are confronted with the predictions of the equation of state (EoS) models allowing for strong first-order phase transition for the mass-radius ( $M$ - $R$ ) diagram. We use models that are based on a covariant density functional (CDF) EoS for nucleonic matter at low densities and a quark matter EoS, parameterized by the speed of sound, at higher densities. To account for the variations in the ellipses for PSR J0030+0451 obtained from different analyses, we examined three scenarios to assess their consistency with our models, focusing particularly on the potential formation of twin stars. We found that in two scenarios, where the ellipses for PSR J0030+0451 and J0437-4715 with masses close to the canonical mass  $\sim 1.4 M_{\odot}$  are significantly separated, our models allow for the presence of twin stars as a natural explanation for potential differences in the radii of these stars.

ArXiv ePrint: [2409.05322](https://arxiv.org/abs/2409.05322)

---

## Contents

<b>1</b>	<b>Introduction</b>	<b>1</b>
<b>2</b>	<b>Models of hybrid stars</b>	<b>2</b>
<b>3</b>	<b>Comparison with astrophysical observations</b>	<b>3</b>
3.1	Scenario A	5
3.2	Scenario B	6
3.3	Scenario C	7
3.4	Tidal deformability and moment of inertia	7
<b>4</b>	<b>Conclusions</b>	<b>8</b>

---

## 1 Introduction

The NICER observations of nearby neutron stars allowed for accurate (up to 10%) inferences of neutron star radii in conjunction with the masses of nearby X-ray-emitting neutron stars. Recent (re)analysis of the data of four millisecond pulsars - the two-solar-mass pulsar PSR J0740+6620 (hereafter J0740) and two canonical mass  $1.4 M_{\odot}$  stars PSR J0437-4715 (hereafter J0437) and J0030+0451 (J0030), and the one-solar-mass pulsar PSR J1231-1411 (J1231) pose a challenge to the modern theories of dense matter to account for the features observed on the mass-radius ( $M$ - $R$ ) diagram of neutron stars. A sharp first-order transition between hadronic and quark matter can produce a disconnected branch of hybrid stars, opening up the possibility of *twin* stars, where there are two different stable configurations, with different radii, but having the same mass. The larger star will be composed entirely of hadronic matter, while the more compact star will be a hybrid star with a quark core in the central region [1–17], for recent reviews see Refs. [18, 19]. Between the hadronic branch and the hybrid branch there is a range of radii for which there are no stable configurations. This is true if the transition from hadronic to quark phase is rapid compared to other time scales in the problem, for example, the period of fundamental modes by which these stars become unstable. In the case of slow conversion, the stability is recovered [20–24].

Recently, new and updated NICER astrophysical constraints have been published for the four pulsars mentioned [25–28]. Notably, the analysis of PSR J0030 resulted in three different ellipses in the  $M$ - $R$  plane, each corresponding to a different analysis model. For PSR J1231, the inference results obtained with the preferred PDT-U model show a strong sensitivity to the choice of radius priors, with stable and likely converged outcomes achieved only under constrained radius priors [27]. The purpose of this paper is to assess the compatibility of these new analyses with the hybrid star models we recently developed in a series of papers [10, 11, 29]. Specifically, we will examine three scenarios, labeled A, B, and C, which share the same data for PSR J0437 and PSR J0740 but incorporate different analyses for PSR J0030 using different models of the surface temperature patterns. The scenarios are defined in Table 1. In model ST-U each of the two hot spots is described by a single spherical cap; in CST+PDT there is a single temperature spherical spot with two components, one emitting and one masking; in ST+PST the primary (ST) is described by a single spherical cap and the secondary (PST) by two components, one emitting and one masking; in ST+PDT the primary (ST) is described by a single spherical cap and the secondary (PDT) by two components, both emitting;

Scenario	J0740	J0437	J1231	J0030		
	ST-U	CST+PDT	PDT-U	ST+PST	ST+PDT	PDT-U
A	×	×	×	×		
B	×	×	×		×	
C	×	×	×			×

**Table 1.** New NICER astrophysical constraints [25–28] used for the three scenarios A, B, C in the present work.

in PDT-U each of the two hot spots is described by two emitting spherical caps. For details see Refs. [25, 28].

In confronting the models of hybrid stars we will pay special attention to the possibility of twin stars in Scenario C, as in this case the data for canonical mass pulsars J0439 and J0030 does not overlap at  $2\sigma$  (95% confidence) level, hinting towards the existence of twin configurations. For this to occur, a strong first-order phase transition is needed, which will be parametrized in terms of the fractional energy density jump  $\Delta\epsilon/\epsilon_{\text{tr}}$ .

The remainder of this work is organized as follows. We briefly describe the physical foundations of the equation of state (EoS) models used in this study in section 2. The theoretical stellar models are compared with astrophysical observations in section 3. Finally, our conclusions are presented in section 4.

## 2 Models of hybrid stars

To ensure this presentation is self-contained, we briefly review the setup from Li et al. [29]. We use four representative nucleonic EoS models based on CDF theory, as discussed in Oertel et al. [30] and Sedrakian et al. [31]. Our models are part of the DDME2 family introduced by Lalazissis et al. [32], but feature varying slope  $L_{\text{sym}}$  of symmetry energy. Our models are labeled as DDLS- $L_{\text{sym}}$ , see Ref. [33]. We keep the skewness constant at the value implied by the parameterization of Ref. [32],  $Q_{\text{sat}} = 479.22$  MeV. Our models share the following nuclear matter parameters: Saturation density  $\rho_{\text{sat}} = 0.152$  fm $^{-3}$ ; Binding energy per particle  $E_{\text{sat}} = -16.14$  MeV at saturation density; Incompressibility  $K_{\text{sat}} = 251.15$  MeV; Symmetry energy  $E_{\text{sym}} = 27.09$  MeV at the crossing density  $\rho_{\text{c}} = 0.11$  fm $^{-3}$ .

In our analysis below we select from the family of DDLS- $L_{\text{sym}}$  two stiff EoS with values of  $L_{\text{sym}} = 80, 100$  MeV and two soft EoS with  $L_{\text{sym}} = 40, 60$  MeV as representative EoS on the basis of which we built our hybrid star models. Note that the EoS of neutron-rich matter below and around  $2\rho_{\text{sat}}$  is dominated by the isovector parameters of a CDF, see for instance Ref. [34], which in the present setup is encoded in  $L_{\text{sym}}$ . The variations of isoscalar parameters, such as  $K_{\text{sat}}$  or  $Q_{\text{sat}}$ , affect the high-density part of the EoS and are unimportant because in our models the hadron-quark phase transition takes place at lower densities, in the range of  $2 \leq \rho/\rho_{\text{sat}} \leq 2.5$ .

The first-order transition to quark matter is parameterized by the baryon density and energy density ( $\rho_{\text{tr}}$  and  $\epsilon_{\text{tr}}$ ) at which the transition occurs, the energy density jump  $\Delta\epsilon$ , and the speed of sound  $c_s$  in the quark matter phase. Following Ref. [29], we first fix  $\rho_{\text{tr}}$  and  $\epsilon_{\text{tr}}$ , and then vary  $\Delta\epsilon$  and  $c_s$ . As described in Ref. [35], we can identify specific values of these parameters that yield a  $M$ - $R$  relation with two disconnected branches. The stars with low central density are purely hadronic, while those with high central density contain a quark core (i.e., hybrid stars) and are separated by an unstable region. This topology could lead to twin configurations, where stars with identical masses differ in their geometric properties such as radii, moments of inertia, and tidal deformabilities.

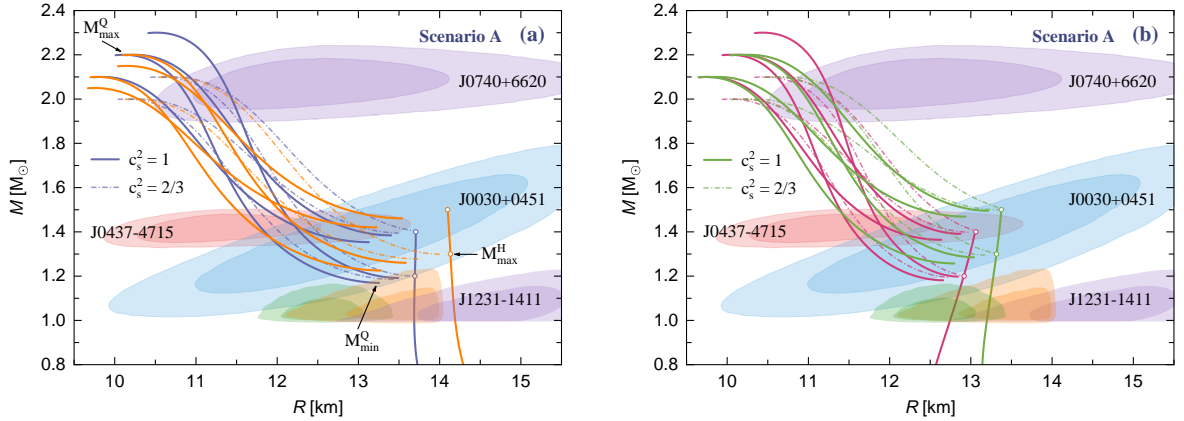


**Figure 1.**  $M$ - $R$  relations for hybrid EoS models with transition mass  $M_{\text{max}}^{\text{H}}$  in the range  $1.2$ - $1.5 M_{\odot}$  and maximum mass  $M_{\text{max}}^{\text{Q}}$  in the range  $2.0$ - $2.3 M_{\odot}$  that were constructed from four representative nucleonic EoS models. Models with stiff nucleonic EoS (DDL-80 and DDL-100) are shown in panel (a), those with soft nucleonic EoS (DDL-40 and DDL-60) in panel (b). Ellipses show observation constraints at 68% and 95% credible levels from analysis of NICER observations according to Refs. [25–28]. The light blue ellipse corresponds to ST+PST analysis for PSR J0030 [25], the three regions for J1231 correspond to PDT-U analysis with three different radius priors [27].

For convenience, we use astrophysical parameters instead of microscopic ones like  $\rho_{\text{tr}}$  and  $\Delta\epsilon$  to characterize a hybrid EoS model, see for illustration panel (a) of Figure 1. These macroscopic parameters are: (a)  $M_{\text{max}}^{\text{H}}$ : the maximum mass of the hadronic branch; (b)  $M_{\text{max}}^{\text{Q}}$ : the maximum mass of the hybrid branch; (c)  $M_{\text{min}}^{\text{Q}}$ : the minimum mass of the hybrid branch. The last quantity allows us to determine the range of masses where twin configurations exist.

As in Ref. [29] we use the constant speed of sound (CSS) parameterization for the quark EoS, which assumes that the speed of sound in quark matter remains constant over the relevant density range. In the extreme high-density limit we expect  $c_s^2 \rightarrow 1/3$  which corresponds to the conformal limit describing weakly interacting massless quarks. The maximum possible speed of sound is the causal limit  $c_s^2 = 1$ . Intermediate values represent varying degrees of stiffness in the quark matter EoS. Below we will explore two possibilities,  $c_s^2 = 1$  and  $2/3$ .

The maximally stiff EoS yields the largest maximum masses for hybrid stars and the maximal difference in the radii of twin stars. The intermediate value is more realistic and mimics what one might expect for non-perturbatively interacting quark matter. Although we will restrict our analysis to the basic CSS model with a single speed of sound over the relevant density range, one could perform a more general analysis using different speeds of sound in different density segments; it is known that this can produce triplets of stars, i.e., three stars with equal masses but different radii [4, 8].

### 3 Comparison with astrophysical observations

We examine hybrid EoS models with transition masses ( $M_{\text{max}}^{\text{H}}$ ) ranging from  $1.2$  to  $1.5$  solar masses. This range encompasses the mass estimation of PSR J0437 reported by Choudhury et al. [28]. Our analysis aims to evaluate the hypothesis that PSR J0437 and J0030 could be twin stars, the first being hadronic and the second hybrid.

We use the following mass and radius measurements:

- PSR J0437-4715: We use the first mass and radius estimates for this brightest pulsar by using the 2017-2021 NICER X-ray spectral-timing data from Choudhury et al. [28]. The preferred

CST+PDT model used informative priors on mass, distance and inclination from PPTA radio pulsar timing data and took into account constraints on the non-source background and validated against XMM-Newton data [28].

- PSR J0030+0451: We use three alternative mass and radius estimates from the reanalysis of 2017-2018 data, as reported by Vinciguerra et al. [25]. One of the estimates is based on the ST+PST NICER-only analysis of the data reported in [36], but uses an improved analysis pipeline and settings. The two other estimates are based on the joint analysis of NICER and XMM-Newton data which are labelled as ST+PDT and PDT-U. The ST+PDT results are more consistent with the magnetic field geometry inferred for the gamma-ray emission for this source [25, 37]. The PDT-U is the most complex model tested in Ref. [25] and is preferred by the Bayesian analysis.
- PSR J0740+6620: We incorporate estimates from Salmi et al. [26], Miller et al. [38], and Riley et al. [39]. The representative estimates used in this study were obtained from a joint NICER and XMM-Newton analysis of the 2018-2022 dataset, based on the preferred ST-U model, which provides a more comprehensive treatment of the background [26].
- PSR J1231-1411: We consider three mass-radius estimates from the preferred PDT-U model with limited radius priors given in Salmi et al. [27]. One estimate limited the radius to be consistent with the previous observational constraints and EoS analyses, and the other two estimates used an uninformative prior, however, the radius was limited to ranges 10-14 km and 8-16 km, respectively. It is important to note, however, that since the radius could not be fully constrained independently in Ref. [27], the possibility of better solutions deviating significantly from the above estimates cannot be excluded.

By combining these observations, we establish three astrophysical scenarios, as detailed in Table 1. This approach enables us to examine different possibilities within the framework of our hybrid EoS models and the mass-twin hypothesis. Notably, the ellipses derived for PSR J0437 significantly overlap with the inferences from GW170817 [40], further reinforcing the selection of EoS based solely on gravitational wave data.

We do not consider the mass and radius estimates for the central compact object in HESS J1731-347, which was characterized as a very low-mass compact star with  $M = 0.77^{+0.20}_{-0.17} M_{\odot}$  and  $R = 10.4^{+0.86}_{-0.78}$  km in Doroshenko et al. [41]. From the theoretical point of view the options to explain this object have been extensively discussed recently and require some assumptions about properties of matter which are difficult to reconcile with the conventional models of dense matter, see for discussions Refs. [11, 29, 42–46]. From the observational point of view, the analysis of Doroshenko et al. [41] has been questioned, in particular their use of the object’s distance and uniform-temperature carbon atmosphere model, see Ref. [47]. It has been also argued that such a model does not perform well on longer-exposure XMM-Newton data from 2014 for the same source. Instead, a model featuring two hot regions emitting blackbody radiation from the surface of a star of mass  $\sim 1.4 M_{\odot}$ , provides a better description of this spectrum [47]. Consequently, there seems to be no consensus from the observational modeling point of view.

Additionally, we note that the companion of the “black widow” pulsar PSR J0952-0607 has been detected in the Milky Way. This pulsar, with a spin frequency of 707 Hz, has a mass estimate of  $M = 2.35^{+0.17}_{-0.17} M_{\odot}$  (68 % credible interval) [48]. Assuming uniform rotation, the increase in the maximum mass configuration due to rotation is approximately  $0.05 M_{\odot}$  [49]. Thus, the lower limit on the mass of J0952 is comparable to that of J0740 at 95% confidence, around  $\sim 2.01 M_{\odot}$ . This provides no additional constraints on our EoS models.

EoS	$\epsilon_{\text{tr}}$ [MeV/fm <sup>3</sup> ]	$\Delta\epsilon/\epsilon_{\text{tr}}$	$M_{\text{max}}^{\text{H}}$ [ $M_{\odot}$ ]	$M_{\text{max}}^{\text{Q}}$ [ $M_{\odot}$ ]	$\Delta M_{\text{twin}}$ [ $M_{\odot}$ ]	$\Delta R_{\text{twin}}$ [km]
DDLS100	300.570	1.0615	1.30	2.10	0.0748	1.84
		0.8881	1.30	2.20	0.0397	1.22
	334.452	1.0055	1.50	2.05	0.0796	1.94
		0.8349	1.50	2.15	0.0389	1.23
DDLS80	300.180	0.8764	1.20	2.20	0.0307	1.01
		0.7249	1.20	2.30	0.0088	0.44
	332.241	0.9100	1.40	2.10	0.0467	1.31
DDLS60	323.965	0.7506	1.40	2.20	0.0162	0.67
		0.9362	1.30	2.10	0.0428	1.14
	356.305	0.7739	1.30	2.20	0.0149	0.59
		0.8252	1.50	2.10	0.0323	0.99
DDLS40	310.074	0.6735	1.50	2.20	0.0049	0.34
		0.8291	1.20	2.20	0.0187	0.61
	338.751	0.6817	1.20	2.30	0.0023	0.15
		0.8856	1.40	2.10	0.0358	0.98
		0.7283	1.40	2.20	0.0089	0.41

**Table 2.** Parameters of the hybrid EoS models used in this work, and the characteristics of their mass-radius curves. All have the maximum sound speed  $c_s^2 = 1$  in the quark phase. The last two columns show the ranges of mass and radius within which twin configurations exist.

### 3.1 Scenario A

Figure 1 shows the  $M$ - $R$  diagrams for hybrid EoS models with four representative nucleonic EoS which are combined with the quark matter EoS specified by two values of the speed of sound  $c_s^2 = 1$  and  $2/3$ . Panel (a) is for stiff nucleonic EoS which demands a strong first-order phase transition with  $M_{\text{max}}^{\text{H}} \lesssim 1.5 M_{\odot}$  in order to be consistent with the NICER inference for PSR J0437. Panel (b) uses soft nucleonic EoS which could match PSR J0437’s inference without a phase transition to quark matter, but still, as an alternative, may allow for phase transitions featuring twin configurations.

Figure 1 demonstrates that Scenario A contains models that are consistent with all four of the  $M$ - $R$  measurements. Each of the curves has a hadronic branch that reaches within the 95% contours for PSR J0030, and a hybrid branch that passes through the 95% contours for J0437 and J0740. (Note that the three contours for PSR J1231 are distinctly different, the stiff hadronic models meet those two larger-radius contours, while soft hadronic models meet those two smaller-radius contours instead.) In several cases the  $M$ - $R$  curves are even consistent with the 68% contours.

For the models with higher transition density, corresponding to  $M_{\text{max}}^{\text{H}} = 1.5 M_{\odot}$  or  $1.4 M_{\odot}$  it is possible that J0030 and J0437 could be hadronic-hybrid twins. For models with a lower transition density ( $M_{\text{max}}^{\text{H}} \lesssim 1.3 M_{\odot}$ ) the mass range where twins exist is below the mass interval of PSR J0437, so that PSR J0030 could be a hadronic or hybrid star, while J0437 must be a hybrid star in this case.

Tables 2 and 3 present the parameters of the used hybrid EoS models with  $c_s^2 = 1$  and  $2/3$ , respectively, in quark phase and characteristics of the corresponding  $M$ - $R$  diagrams, i.e., the values of  $M_{\text{max}}^{\text{H}}$ ,  $M_{\text{max}}^{\text{Q}}$ , and ranges of mass and radius that characterize twin configurations,  $\Delta M_{\text{twin}} = M_{\text{max}}^{\text{H}} - M_{\text{min}}^{\text{Q}}$ , and  $\Delta R_{\text{twin}}$  the radius difference between the  $M_{\text{max}}^{\text{H}}$  hadronic star and that of the hybrid counterpart with the same mass. Note that the case  $c_s^2 = 1$  allows us to establish the maximum range where twin configurations exist in our setup.

EoS	$\epsilon_{\text{tr}}$ [MeV/fm <sup>3</sup> ]	$\Delta\epsilon/\epsilon_{\text{tr}}$	$M_{\text{max}}^{\text{H}}$ [ $M_{\odot}$ ]	$M_{\text{max}}^{\text{Q}}$ [ $M_{\odot}$ ]	$\Delta M_{\text{twin}}$ [ $M_{\odot}$ ]	$\Delta R_{\text{twin}}$ [km]
DDL100	300.570	0.7823	1.30	2.00	0.0225	0.92
		0.6298	1.30	2.10	0.0015	0.21
	334.452	0.6898	1.50	2.00	0.0124	0.69
		0.5467	1.50	2.10	-	-
DDL80	300.180	0.7641	1.20	2.00	0.0148	0.64
		0.6125	1.20	2.10	-	-
	332.241	0.6735	1.40	2.00	0.0059	0.41
DDL60	323.965	0.5313	1.40	2.10	-	-
		0.6851	1.30	2.00	0.0045	0.29
	356.305	0.5414	1.30	2.10	-	-
		0.6198	1.50	2.00	0.0006	0.14
DDL40	310.074	0.4826	1.50	2.10	-	-
		0.7256	1.20	2.00	0.0063	0.31
	338.751	0.5777	1.20	2.10	-	-
		0.6573	1.40	2.00	0.0014	0.18
		0.5166	1.40	2.10	-	-

**Table 3.** Same as Table 2 but for models have the intermediate sound speed  $c_s^2 = 2/3$  in the quark phase.

### 3.2 Scenario B

This is the scenario where the  $M$ - $R$  ellipses for canonical mass stars PSR J0030 and J0437 are maximally overlapping; see Figure 2. In this case, hadronic stars are consistent with data only at  $2\sigma$  (95% confidence) level, and only for soft hadronic matter (panel b). If the hadronic EoS is stiff then both stars must be hybrid which means they may have hadronic twins with significantly larger radii  $R \geq 13.7$  km (the  $2\sigma$  upper limit for J0437) in our example, see panel (a).

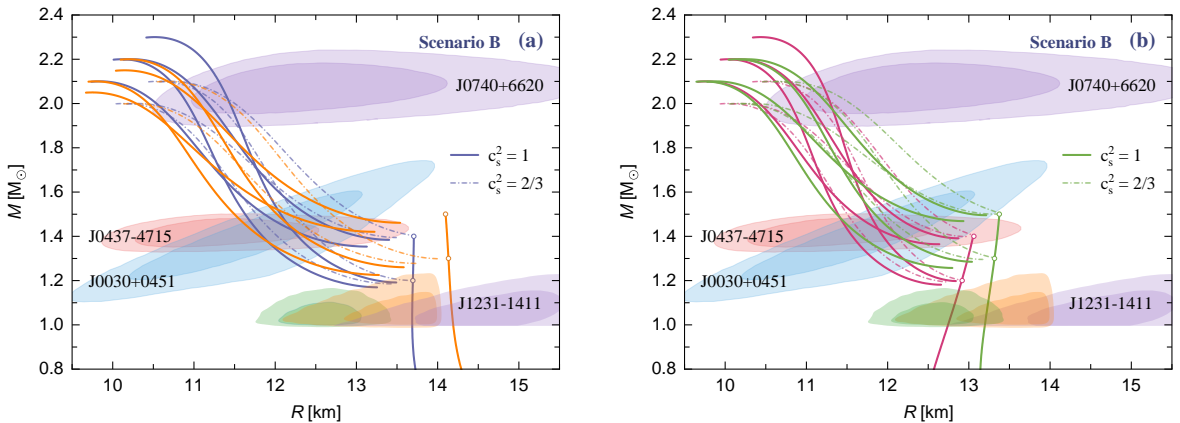


**Figure 2.** Same as Figure 1, but for scenario B, where the light blue ellipse corresponds to ST+PDT analysis for PSR J0030 [25].



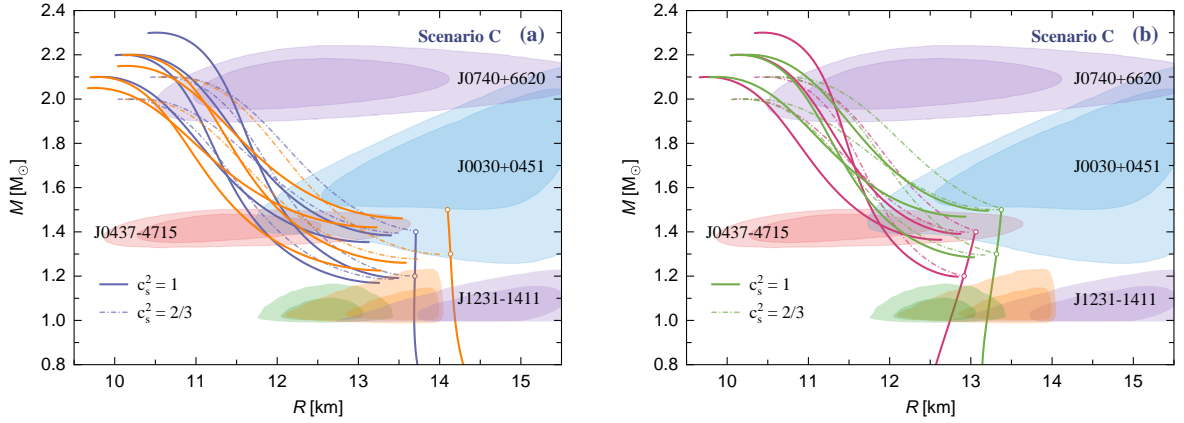


**Figure 3.** Same as Figure 1, but for scenario C, where the light blue ellipse corresponds to PDT-U analysis for PSR J0030 [25].

### 3.3 Scenario C

This is the scenario where the  $M$ - $R$  ellipses for PSR J0030 and J0437 overlap only at  $2\sigma$  (95% confidence), see Figure 3. This scenario can be viewed as a more extreme version of Scenario A, therefore, the conclusions drawn above apply to this scenario too. Nevertheless, there are some quantitative differences. PSR J0030 has now a large radius  $R > 12$  km, which excludes models of EoS with soft hadronic matter which produce low values of  $M_{\max}^H$  or  $M_{\max}^Q$  with  $R_{1.4} < 12$  km (the  $2\sigma$  lower limit for J0030), where  $R_{1.4}$  is the radius of  $1.4 M_{\odot}$  star. This is the case, for example, for the EoS based on DDLS-60 ( $M_{\max}^H = 1.3 M_{\odot}$ ,  $M_{\max}^Q = 2.1 M_{\odot}$  and  $c_s^2 = 1$ ) and DDLS-40 ( $M_{\max}^H = 1.2 M_{\odot}$ ,  $M_{\max}^Q = 2.0 M_{\odot}$  and  $c_s^2 = 2/3$ ).

### 3.4 Tidal deformability and moment of inertia

In this section, we consider two additional integral parameters of hybrid stars that have observational significance - the tidal deformability and moment of inertia. Figure 4 (a) shows the dimensionless

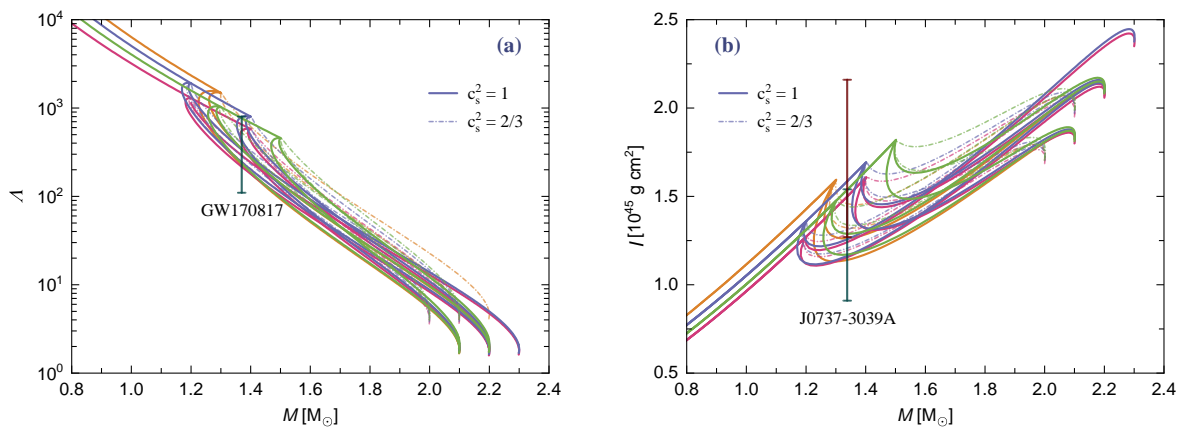


**Figure 4.** Mass-tidal deformability (left panel) and mass-moment of inertia (right panel) relations for EoS models. The 90% confidence ranges for a  $1.362 M_{\odot}$  star deduced from the analysis of GW170817 [40] (left panel) and for  $1.338 M_{\odot}$  PSR J0737-3039 A from radio observations [50] (right panel) are shown with the vertical error bars.



tidal deformability vs mass relation for our models. It is seen that the models discussed in this work satisfy the constraint placed for a  $1.362 M_{\odot}$  star from the analysis of the GW170817 event [40]. It is also seen that the softer EoS safely passes through the required range for  $\Lambda_{1.362}$ . Furthermore, for hybrid models for which  $M_{\min}^Q \leq 1.4 M_{\odot}$  the transition to quark matter improves the agreement with the data.

Figure 4 (b) shows the moment of inertia predicted by EoS models for  $1.338 M_{\odot}$  star. A motivation for considering the moment of inertia comes from the observation of binary PSR J0737-3039 A [50, 51], which shows changes in orbital parameters, such as the orbit inclination (the angle between the orbital plane and observer’s line of sight) and the periastron position [52]. It is evident from the figure that our models of hybrid stars are broadly consistent with the constraint  $0.91 \leq I_{1.338} \leq 2.16$  inferred from 16-yr data span reported in Ref. [50], where  $I_{1.338}$  is the moment of inertia of a neutron star with  $1.338 M_{\odot}$  mass in units of  $10^{45} \text{g cm}^2$ .

## 4 Conclusions

Motivated by the recent (re)analysis of the data on two X-ray emitting pulsars PSR J0030+0451 and J0470+6620 as well as new results on PSR J0437-4715 and J1231-1411 we compared the new ellipses in the  $M$ - $R$  diagram for these pulsars with our models of hybrid stars, which are based on CDF EoS for nucleonic matter at low densities and quark matter EoS, parametrized by speed of sound, at higher densities. These models are also validated by comparisons of their predicted tidal deformabilities with the observations of GW170817 and predicted moment of inertia with the constraints for PSR J0737-3039 A, see Figure 4.

In more detail, we considered three possible scenarios A, B and C which correspond to the three mass and radius estimates taken from a reanalysis of 2017-2018 data [25] for PSR J0030+0451. These include an improved NICER-only ST+PST analysis and two joint NICER-XMM-Newton models (ST+PDT and PDT-U), with the Bayesian-preferred PDT-U being the most complex. We then examined the consistency of the three scenarios with our models with a special focus on the possibility of the formation of twin stars. We find that in two scenarios (A and C), where the ellipses for the canonical mass ( $\sim 1.4 M_{\odot}$ ) stars J0030+0451 and J0437-4715 exhibit the maximal mismatch, the potential difference in the radii of these stars within these scenarios is naturally explained by the presence of twin stars.

To conclude, the ability of the hybrid star models to explain observational data from multiple sources (X-ray pulsars and gravitational waves) encourages further refinement of theoretical models, potentially leading to more accurate descriptions of neutron star interiors. This can be only achieved through combining theoretical models (for example using the classes of models discussed here) with observational data, which is expected to improve over time.

## Acknowledgments

J. L. is supported by the National Natural Science Foundation of China under Grant No. 12105232 and the Fundamental Research Funds for the Central Universities under Grant No. SWU-020021. A. S. is funded by Deutsche Forschungsgemeinschaft Grant No. SE 1836/5-3 and the Polish NCN Grant No. 2023/51/B/ST9/02798. M. A. is partly supported by the U.S. Department of Energy, Office of Science, Office of Nuclear Physics under Award No. DE-FG02-05ER41375.

## References

- [1] N. K. Glendenning and C. Kettner, *Nonidentical neutron star twins*, *Astron. Astrophys.* **353** (2000) L9, [[astro-ph/9807155](#)].
- [2] J. L. Zdunik and P. Haensel, *Maximum mass of neutron stars and strange neutron-star cores*, *Astron. Astrophys.* **551** (2013) A61, [[1211.1231](#)].
- [3] S. Benic, D. Blaschke, D. E. Alvarez-Castillo, T. Fischer and S. Typel, *A new quark-hadron hybrid equation of state for astrophysics - I. High-mass twin compact stars*, *Astron. Astrophys.* **577** (2015) A40, [[1411.2856](#)].
- [4] M. Alford and A. Sedrakian, *Compact Stars with Sequential QCD Phase Transitions*, *Phys. Rev. Lett.* **119** (Oct., 2017) 161104, [[1706.01592](#)].
- [5] D. E. Alvarez-Castillo, D. B. Blaschke, A. G. Grunfeld and V. P. Pagura, *Third family of compact stars within a nonlocal chiral quark model equation of state*, *Phys. Rev. D* **99** (2019) 063010, [[1805.04105](#)].
- [6] D. Blaschke, A. Ayriyan, D. E. Alvarez-Castillo and H. Grigorian, *Was GW170817 a Canonical Neutron Star Merger? Bayesian Analysis with a Third Family of Compact Stars*, *Universe* **6** (2020) 81, [[2005.02759](#)].
- [7] J.-E. Christian and J. Schaffner-Bielich, *Confirming the Existence of Twin Stars in a NICER Way*, *Astrophys. J.* **935** (2022) 122, [[2109.04191](#)].
- [8] J. J. Li, A. Sedrakian and M. Alford, *Relativistic hybrid stars with sequential first-order phase transitions and heavy-baryon envelopes*, *Phys. Rev. D* **101** (2020) 063022, [[1911.00276](#)].
- [9] J. J. Li, A. Sedrakian and M. Alford, *Relativistic hybrid stars in light of the NICER PSR J0740+6620 radius measurement*, *Phys. Rev. D* **104** (2021) L121302, [[2108.13071](#)].
- [10] J. J. Li, A. Sedrakian and M. Alford, *Relativistic Hybrid Stars with Sequential First-order Phase Transitions in Light of Multimessenger Constraints*, *Astrophys. J.* **944** (2023) 206, [[2301.10940](#)].
- [11] J. J. Li, A. Sedrakian and M. Alford, *Ultracompact hybrid stars consistent with multimessenger astrophysics*, *Phys. Rev. D* **107** (2023) 023018, [[2207.09798](#)].
- [12] P. Laskos-Patkos, P. S. Koliogiannis and C. C. Moustakidis, *Hybrid stars in light of the HESS J1731-347 remnant and the PREX-II experiment*, *Phys. Rev. D* **109** (2024) 063017, [[2312.07113](#)].
- [13] M. Naseri, G. Bozzola and V. Paschalidis, *Exploring pathways to forming twin stars*, *Phys. Rev. D* **110** (2024) 044037, [[2406.15544](#)].
- [14] J. C. Jiménez, L. Lazzari and V. P. Gonçalves, *How the QCD trace anomaly behaves at the core of twin stars?*, *arXiv e-prints* (2024), [[2408.11614](#)].
- [15] N.-B. Zhang and B.-A. Li, *Impact of the nuclear equation of state on the formation of twin stars*, *arXiv e-prints* (2024), [[2406.07396](#)].
- [16] Y. Kini, T. Salmi, S. Vinciguerra et al., *Pulse Profile Modelling of Thermonuclear Burst Oscillations III : Constraining the properties of XTE J1814-338*, *arXiv e-prints* (2024), [[2405.10717](#)].
- [17] P. Laskos-Patkos, G. A. Lalazissis, S. Wang, J. Meng, P. Ring and C. C. Moustakidis, *Speed of sound bounds and first-order phase transitions in compact stars*, *arXiv e-prints* (2024), [[2408.15056](#)].
- [18] G. Baym, T. Hatsuda, T. Kojo, P. D. Powell, Y. Song and T. Takatsuka, *From hadrons to quarks in neutron stars: a review*, *Rep. Prog. Phys.* **81** (2018) 056902, [[1707.04966](#)].
- [19] A. Sedrakian, *Impact of Multiple Phase Transitions in Dense QCD on Compact Stars*, *Particles* **6** (2023) 713–730, [[2306.13884](#)].
- [20] P. B. Rau and A. Sedrakian, *Two first-order phase transitions in hybrid compact stars: Higher-order multiplet stars, reaction modes, and intermediate conversion speeds*, *Phys. Rev. D* **107** (2023) 103042, [[2212.09828](#)].

- [21] P. B. Rau and G. G. Salaben, *Nonequilibrium effects on stability of hybrid stars with first-order phase transitions*, *Phys. Rev. D* **108** (2023) 103035, [2309.08540].
- [22] C. H. Lenzi, G. Lugones and C. Vasquez, *Hybrid stars with reactive interfaces: Analysis within the Nambu-Jona-Lasinio model*, *Phys. Rev. D* **107** (2023) 083025, [2304.01898].
- [23] I. F. Ranea-Sandoval, M. Mariani, M. O. Celi, M. C. Rodríguez and L. Tonetto, *Asteroseismology using quadrupolar  $f$ -modes revisited: Breaking of universal relationships in the slow hadron-quark conversion scenario*, *Phys. Rev. D* **107** (2023) 123028, [2306.02823].
- [24] I. A. Rather, K. D. Marquez, B. C. Backes, G. Panotopoulos and I. Lopes, *Radial oscillations of hybrid stars and neutron stars including delta baryons: the effect of a slow quark phase transition*, *Jour. Cosmo. Astropart. Phys.* **05** (2024) 130, [2401.07789].
- [25] S. Vinciguerra, T. Salmi, A. L. Watts et al., *An Updated Mass–Radius Analysis of the 2017–2018 NICER Data Set of PSR J0030+0451*, *Astrophys. J.* **961** (2024) 62, [2308.09469].
- [26] T. Salmi, D. Choudhury, Y. Kini et al., *The Radius of the High-mass Pulsar PSR J0740+6620 with 3.6 yr of NICER Data*, *Astrophys. J.* **974** (2024) 294, [2406.14466].
- [27] T. Salmi, J. S. Deneva, P. S. Ray et al., *A NICER View of PSR J1231–1411: A Complex Case*, *Astrophys. J.* **976** (2024) 58, [2409.14923].
- [28] D. Choudhury, T. Salmi, S. Vinciguerra et al., *A NICER View of the Nearest and Brightest Millisecond Pulsar: PSR J0437–4715*, *Astrophys. J. Lett.* **971** (2024) L20, [2407.06789].
- [29] J. J. Li, A. Sedrakian and M. Alford, *Hybrid Star Models in the Light of New Multimessenger Data*, *Astrophys. J.* **967** (2024) 116, [2401.02198].
- [30] M. Oertel, M. Hempel, T. Klähn and S. Typel, *Equations of state for supernovae and compact stars*, *Rev. Mod. Phys.* **89** (2017) 015007, [1610.03361].
- [31] A. Sedrakian, J. J. Li and F. Weber, *Heavy baryons in compact stars*, *Prog. Part. Nucl. Phys.* **131** (2023) 104041, [2212.01086].
- [32] G. A. Lalazissis, T. Niksic, D. Vretenar and P. Ring, *New relativistic mean-field interaction with density-dependent meson-nucleon couplings*, *Phys. Rev. C* **71** (2005) 024312.
- [33] J. J. Li and A. Sedrakian, *New covariant density functionals of nuclear matter for compact star simulations*, *Astrophys. J.* **957** (2023) 41, [2308.14457].
- [34] J. J. Li and A. Sedrakian, *Baryonic models of ultra-low-mass compact stars for the central compact object in HESS J1731–347*, *Phys. Lett. B* **844** (2023) 138062, [2306.14185].
- [35] M. G. Alford, S. Han and M. Prakash, *Generic conditions for stable hybrid stars*, *Phys. Rev. D* **88** (2013) 083013, [1302.4732].
- [36] T. E. Riley, A. L. Watts, S. Bogdanov et al., *A NICER View of PSR J0030+0451: Millisecond Pulsar Parameter Estimation*, *Astrophys. J. Lett.* **887** (2019) L21, [1912.05702].
- [37] C. Kalapotharakos, Z. Wadiasingh, A. K. Harding and D. Kazanas, *The Multipolar Magnetic Field of Millisecond Pulsar PSR J0030+0451*, *Astrophys. J.* **907** (2021) 63, [2009.08567].
- [38] M. C. Miller, F. Lamb, A. J. Dittmann et al., *The Radius of PSR J0740+6620 from NICER and XMM-Newton Data*, *Astrophys. J. Lett.* **918** (2021) L28, [2105.06979].
- [39] T. E. Riley, A. L. Watts, P. S. Ray et al., *A NICER View of the Massive Pulsar PSR J0740+6620 Informed by Radio Timing and XMM-Newton Spectroscopy*, *Astrophys. J. Lett.* **918** (2021) L27, [2105.06980].
- [40] LIGO SCIENTIFIC, VIRGO collaboration, B. P. Abbott, R. Abbott, T. D. Abbott et al., *GW170817: Measurements of neutron star radii and equation of state*, *Phys. Rev. Lett.* **121** (2018) 161101, [1805.11581].

- [41] V. Doroshenko, V. Suleimanov, G. Pühlhofer and A. Santangelo, *A strangely light neutron star within a supernova remnant*, *Nature Astron.* **6** (2022) 1444–1451.
- [42] L. Brodie and A. Haber, *Nuclear and hybrid equations of state in light of the low-mass compact star in HESS J1731-347*, *Phys. Rev. C* **108** (2023) 025806, [2302.02989].
- [43] S. Kubis, W. Wójcik, D. A. Castillo and N. Zabari, *Relativistic mean-field model for the ultracompact low-mass neutron star HESS J1731-347*, *Phys. Rev. C* **108** (2023) 045803, [2307.02979].
- [44] V. Sagun, E. Giangrandi, T. Dietrich, O. Ivanytskyi, R. Negreiros and C. Providência, *What Is the Nature of the HESS J1731-347 Compact Object?*, *Astrophys. J.* **958** (2023) 49, [2306.12326].
- [45] B. Gao, Y. Yan and M. Harada, *Reconciling constraints from the supernova remnant HESS J1731-347 with the parity doublet model*, *Phys. Rev. C* **109** (2024) 065807, [2404.04786].
- [46] M. Veselsky, P. S. Koliogiannis, V. Petousis, J. Leja and C. C. Moustakidis, *How the HESS J1731-347 event could be explained using  $\mathbf{K}^-$  condensation*, *arXiv e-prints* (2024) , [2410.05083].
- [47] J. A. J. Alford and J. P. Halpern, *Do Central Compact Objects have Carbon Atmospheres?*, *Astrophys. J.* **944** (2023) 36, [2302.05893].
- [48] R. W. Romani, D. Kandel, A. V. Filippenko, T. G. Brink and W. Zheng, *PSR J0952–0607: The Fastest and Heaviest Known Galactic Neutron Star*, *Astrophys. J. Lett.* **934** (2022) L17, [2207.05124].
- [49] J. J. Li, A. Sedrakian and F. Weber, *Universal relations for compact stars with heavy baryons*, *Phys. Rev. C* **108** (2023) 025810, [2306.14190].
- [50] M. Kramer, I. H. Stairs, R. N. Manchester et al., *Strong-field gravity tests with the double pulsar*, *Phys. Rev. X* **11** (2021) 041050, [2112.06795].
- [51] M. Burgay, N. D’Amico, A. Possenti et al., *An increased estimate of the merger rate of double neutron stars from observations of a highly relativistic system*, *Nature* **426** (2003) 531–533, [astro-ph/0312071].
- [52] J. M. Lattimer and B. F. Schutz, *Constraining the Equation of State with Moment of Inertia Measurements*, *Astrophys. J.* **629** (2005) 979–984, [astro-ph/0411470].